MSUCL-202
January 1976

A High Resolution Study of ^{26}Al via the (p,d) Reaction*

D.L. Show, B.H. Wildenthal, J.A. Nolen, Jr., and E. Kashy

Cyclotron Laboratory and Department of Physics
Michigan State University, East Lansing, Michigan 48824

ABSTRACT

Excitation energies and angular distributions of ^{26}Al levels in the first 6 MeV of excitation have been measured with the ^{27}Al(p,d)^{26}Al reaction at E_p=35 MeV. Deuteron spectra were analyzed with an Enge split-pole magnetic spectrograph and recorded on nuclear emulsions (experimental resolution $\tilde{=}$6 keV, FWHM); supplementary data were recorded with position-sensitive wire proportional counters. The angular distributions were analyzed with the DWBA to extract the ℓ-values and associated spectroscopic factors of the neutron transfers. The results for excitation energies, ℓ-values, spectroscopic factors, and values of J^π,T are discussed in terms of previous experimental and theoretical work and in the light of new shell-model calculations for this system.

[NUCLEAR REACTIONS ^{27}Al(p,d), E=35 MeV; measured $\sigma(\theta)$, excitation energies. ^{26}Al deduced ℓ, spectroscopic factors. Magnetic spectrograph.]

*Research supported by the U.S. National Science Foundation.

I. INTRODUCTION

The structure of the energy levels of ^{26}Al is enigmatic. In terms of the simplest shell model, based on an ^{16}O core, the active system consists of 5 protons and 5 neutrons, each in the $d_{5/2}$ orbit. In such a model, ^{26}Al could be treated as coupling of single neutron and proton holes in the $d_{5/2}$ orbit. However, there is no simple relationship between the lowest observed states of ^{26}Al and those of its particle conjugate in the $d_{5/2}^n$ model, ^{18}F.[1] Simple rotational-model schemes[2] fare no better than the simplest shell-model analysis and the addition of considerable complexity to the rotational model, by considering several bands and extensive band-mixing via Coriolis coupling, still fails to yield a viable explanation of this system.[3] Shell-model calculations which involve both the $d_{5/2}$ and $s_{1/2}$ orbits,[4] and which quantitatively explain many features of the A=20-28 region still fail to give even a qualitative representation of the T=0 part of the level structure of ^{26}Al. In doubly-odd, self-conjugate nuclei such as ^{26}Al, T=0 and T=1 levels both occur in the first few MeV of excitation. The isobaric analogues of the T=1 levels of ^{26}Al which occur in ^{26}Mg have been studied in some detail,[5] and while the A=20-28 shell model analysis of Ref. 4 can explain some features of this subset of levels, particularly the ^{27}Al-^{26}Mg proton pickup data,[6,7] a complete understanding of even just the T=1 levels has also been lacking.

The confused situation in which the theory of the structure of ^{26}Al has existed has not inhibited experimental study of the

nucleus. A succession of investigations concentrating on the gamma decays of the excited states[8-21] and the ^{26}Si β-decay[22] have established an almost complete set of levels up through 4 MeV of excitation, assigned or delimited many J^{π} values and measured some lifetimes and electromagnetic transition strengths for these levels. Particle-transfer studies of ^{26}Al have been made with the $(^3He,d)^{23,24,25}$, $(d,n)^{25,26}$, $(^3He,p)^{27,28}$, $(\alpha,d)^{29}$, $(p,d)^{30,31,32}$, and $(^3He,\alpha)^{28,33}$ reactions. As mentioned previously, the analogsof the T=1 levels have been studies in ^{26}Mg via the (d,He^3) reaction on ^{27}Al.[7,34]

The first aim of the present experiment was to make as complete and accurate a catalog of the energy levels of ^{26}Al as was feasible with nucleon-transfer-reaction techniques. To this end, multiple spectra covering the first 6 MeV of excitation were recorded with both good energy resolution and good counting statistics. The second aim was to measure the angular variations of the transition intensities at angles for which the various characteristic shapes of different orbital angular momentum transfers are most distinct, thus maximizing the accuracy of the ℓ-values and spectroscopic factors assigned to the observed levels via DWBA analysis of the data. The results obtained are compared to the relevant predictions of new shell-model calculations for A=26 in which some of the deficiencies of the previous theoretical studies of this system are removed.

II. EXPERIMENTAL PROCEDURE

The collection of data was carried out in two phases, both of which used the 35 MeV proton beam from the MSU Cyclotron and an

Enge split-pole magnetic spectrograph. In the first phase, a thin ^{27}Al target was used and the deuterons were detected in Kodak NTB 25 micron nuclear emulsions placed in the focal plane of the spectrograph. The target was prepared by vacuum evaporation of a layer of Al about 60 μg/cm^2 thick onto a 30 μg/cm^2 carbon foil stretched over a 1.5 cm diameter hole in an (aluminum) target frame. Spectra were taken between θ_L=4° and 52°, with long and short exposures made at each angle to provide accurate counts for both weak and strong peaks. The plates were scanned by human scanners with the help of a computer-linked microscope system. Using dispersion matching[35] and a previously described[36] resolution-optimization procedure, an average energy resolution for detected deuteron groups of 6 keV, FWHM, was obtained for these emulsion data. The spectrum measured at 22° is shown in Fig. 1.

In the second phase of the experiment, a thicker ^{27}Al target was used and the deuterons were detected with a position-sensitive single-wire proportional counter.[37] The target was a self-supporting foil of aluminum prepared by rolling 0.3 mil aluminum down to 0.1 mil thickness. The wire counter was operated in coincidence with a second, similar, counter placed behind it, in order to reduce background as described in Reference 37. Signals from the counter were fed into a Sigma-7 computer in which on-line particle identification and storage of both the deuteron and triton spectra were performed. This technique allowed rapid accumulation of data with high statistical accuracy

and was most valuable for the many states below 4 MeV which are separated from each other by more than the resolution of ~50 keV, FWHM achieved with the counter. In this part of the experiment, spectra were measured from 3° to 80° in the laboratory system. Data acquisition was monitored by reference both to the collected beam charge and to the number of protons elastically scattered into a monitor detector (NaI) placed at 90° to the beam direction. The two resultant normalizations agreed with each other to 2% on the average. The angular distributions measured with nuclear emulsions were normalized to those measured with the wire counter by matching up the distributions of the lowest few states.

The overall cross section normalization for the (p,d) data was obtained by comparison of the (p,d) counting rates to those for proton elastic scattering at six angles between 25° and 50°. These comparison measurements were made with a single experimental configuration of target, charge collector, and monitor detector, and used the position-sensitive wire proportional counter as the particle detector. We assume that the differential cross sections for elastic scattering at these angles are equal to those predicted in an optical model calculation which use the parameters of Becchetti and Greenlees.[38] (See Table 3). For these angles, and for ^{27}Al, the uncertainty in the optical-model predictions is perhaps 10%. (The relative shape of the calculated distribution fits our six point measured distribution.) The uncertainty in the mechanics of our normalization procedure is also approximately 10%, leading to approximately a 15% overall

uncertainty in the cross section normalization for the (p,d) data. The results of the differential cross section measurements are presented in Figs. 3-6.

III. DATA ANALYSIS

1. Excitation Energies

One of the goals of the experiment was to firmly establish the correspondence between the energy levels of ^{26}Al observed in charged particle reactions and gamma-ray studies by measuring as accurately as possible the excitation energies for the states below 6 MeV of excitation. A recent (p,γ) study has established accurate ($\leq$ 2 keV) excitation energies for most states below 6 MeV excitation in ^{26}Al but there currently exist no charged particle data of comparable precision. The excitation energy assignments made in the present work are derived from the high-resolution nuclear-emulsion data. The exposed emulsions were scanned up to the group corresponding to the ^{12}C(p,d) ground state, which corresponds to about 6 MeV of excitation in ^{26}Al. In addition, the positions of the centroids of strong peaks falling between the position of the ^{12}C(p,d) ground state group and the low-momentum end of the second plate were also measured. The spectra obtained from scanning the emulsions were input to a computer program which fit a gaussian shape derived from one peak with good statistics to all of the peaks and calculated centroid positions and peak areas. The areas were later used in determining the angular distributions.

The momentum vs. displacement function (ρ vs. D curve) for our spectrograph is known to be almost linear, with a small quadratic correction term.[39] However, the coefficients of the linear and quadratic terms vary with the orientation of the plate holder, which is in turn varied for different angles of measurement in order to achieve the best energy resolution. We therefore use a procedure for calculating excitation energies which determines the coefficients for these terms at each angle based on a least-squares fit to certain reference peaks on the plate.[39] The peaks used correspond to the states listed in Table 1. The excitation energies and Q-values of these states and reactions are well known,[5,39,40] and the positions of the corresponding particle groups are well spaced out along the plates. In addition to determining the coefficients of the ρ vs. D curve, this procedure determines corrections for uncertainties in the beam energy, magnetic field, and scattering angle. The energies of the other states in ^{26}Al are then determined by this calibration and reaction kinematics. The spectra at 4°, 11°, and 22° were each analyzed in this way and the results averaged to give the final energies. This procedure yields an uncertainty of 1-3 keV in the assigned values of excitation energy below 6 MeV excitation. The excitation energies of states in ^{26}Al determined in the present experiment are compared with previous gamma-ray determinations in Table 2. The weighted averages of the present and previous measurements are also given in the table.

The question of whether or not a particular level was observed in our data was resolved by cross checking between high resolution

spectra measured at several different angles and also by reference to the spectra measured with very good counting statistics with the wire counter. We should have detected, at a minimum, any previously observed isolated level ($\geq$15 keV from nearest peak) populated with a cross section $\geq$4 μb/sr, and any new, similarily isolated, level populated with the cross section $\geq$10 b/sr. Doublets of comparable strength would be detected if their separation was $\geq$5 keV. The separation via peak fitting of a 6 keV doublet with a yield ratio of about 3:1 is illustrated in Figure 2.

2. Angular Distributions

The angular distributions of the (p,d) reaction to the observed states of ^{26}Al are shown in Figs. 3-6. The curves in these figures result from distorted-waves Born approximation calculations made with the code DWUCK.[41] In these calculations, the Becchetti-Greenlees[38] optical model parameters were used for the proton channel and the parameters for the deuteron channel were calculated by beginning with the prescription given by Satchler[42] for using the Johnson-Soper adiabatic model.[43,44] (The neutron and proton optical model parameters needed for this procedure was also taken from Becchetti and Greenlees.[38]) The values for the deuteron parameters resulting from Satchler's formulae were then altered by decreasing the magnitude of the real well depth by 4% and increasing the imaginary well radius from 1.29 F to 1.35 F. These parameters, listed in Table 3 as Set A, gave the best overall fit for all ℓ-transfer and Q-values, and were used to determine the spectroscopic factors given in this paper.

In addition to the adiabatic-model deuteron parameters we tried other sets of deuteron parameters based on deuteron elastic scattering. The deuteron parameters listed in Table 3 as Set B were obtained by Hinterberger, et al.[45] Sample calculations with these parameters are shown in Fig. 7 for two different excitation energies. The curves are normalized to $C^2S=1$, and hence illustrate the Q-dependence of both the magnitudes and shapes of the DWBA calculations.

The curves in Figure 7 also give some idea of the parameter dependence of both the absolute and relative values extracted for C^2S. Inspection of the figure indicates that the portions of the curves near the "stripping maxima" (0° for $\ell=0$ and 20° for $\ell=2$) are the least parameter dependent. This is consistent with the generally accepted idea that the DWBA is most reliable at these maxima. Using this prescription leads to a 20% difference in the absolute C^2S determined by the parameter sets A and B. The absolute spectroscopic factors for the $\ell=0$ transitions are more parameter dependent and they are particularly sensitive to whether the normalization is done near the primary or secondary stripping maximum.

For a reaction such as $^{27}Al(p,d)^{26}Al$, in which the target spin is not zero ($J^\pi=5/2^+$ for ^{27}Al ground state), many of the final states ($J^\pi=2^+$ and 3^+) can be populated by a combination of $\ell=0$ and $\ell=2$ transfer. The problem is further complicated in ^{26}Al in the present instance because the observed $\ell=2$ shape exhibits a stronger Q-dependence than is predicted by any of the parameters we have used. (We have chosen parameters which fit the higher-lying $\ell=2$ transitions better than the lower-lying ones in order to have good shapes for the region where we observe most mixed ℓ-transfers.) Even so, because $\ell=2$ transfer has both

less structure and a smaller intrinsic average cross section than does that for $\ell=0$, we can in many cases only set an upper limit on the strength of the $\ell=2$ component in transitions which are predominantly $\ell=0$.

The experimental spectroscopic factors were extracted by taking the ratios of the experimental cross sections to the DWBA predictions and multiplying by the appropriate factors.[41] In calculating the $\ell=2$ spectroscopic factors it was assumed that the transferred neutron was from the $1d_{5/2}$ orbit rather than $1d_{3/2}$ orbit for all $\ell=2$ transitions. If the neutron transferred in a given $\ell=2$ transition was indeed from the $1d_{3/2}$ orbit instead of the $1d_{5/2}$ orbit as we assumed, then our spectroscopic factor would be too small by a factor of 1.2. We made a similar assumption for the $\ell=1$ transfers, for which we assumed that $1p_{1/2}$ neutron was picked up.

In fitting the theoretical distributions to the experimental shapes we used a least-squares technique which covered only the angles from 4°-35° to determine the magnitude of each ℓ-component. These forward angles are less sensitive to the particular parameters used in the DWBA. For the low lying $\ell=2$ transitions the angles near the stripping maximum (20°) were heavily weighted in the normalization. The fits obtained are shown in Figs. 3-6. The solid curves are the sum of the spectroscopic factor-weighted DWBA predictions. Where mixed ℓ-transfer are assigned, the individual ℓ-transfer contributions are shown with dotted curves.

IV. RESULTS

1. Excitation energies of states in ^{26}Al.

The weighted averages of the excitation energies for states of ^{26}Al seen in the present experiment and in previous γ-ray experiments, are given in Table 2. Except for the unresolved 3 keV triplet at 2069 keV and the unresolved 4 keV doublet at 3751 keV we have observed all but 3 previously known states in ^{26}Al below 5.85 MeV excitation energy. Six of the 58 states listed in Table 2 did not have accurate excitation energies assigned from gamma-ray work. In the cases where a comparison can be made, the current assignments of excitation energies based on the calibration lines listed in Table 1 are in very good agreement with the gamma-ray determinations.

2. Spin and ℓ-value assignments in ^{26}Al.

The existing spin assignments or limits for states of ^{26}Al are listed in Table 4. There are firm spin and parity assignments via gamma-ray work for most of the states below 4 MeV, but there are few such assignments for higher lying states. There are several states above 4 MeV for which parity assignments and spin limitations can be made from direct particle-transfer reaction work. These assignments are based on ℓ_p determinations from $(^3He,d)^{24}$ and $(d,n)^{25,26}$ reactions and ℓ_n determinations from $(p,d)^{32}$ and $(^3He,\alpha)^{33}$ reactions, with some further evidence provided by L-transfer measurements with the $(^3He,p)^{27}$ reaction. The experimental angular distributions from the current (p,d)

study at 35 MeV are shown together with DWBA calculations in figures 3-6, where the ℓ-values of the picked-up neutrons are also indicated for each state observed. In a (p,d) study at 20 MeV Kroon, et al.[32] determined ℓ-values for 13 states of ^{26}Al below 4.7 MeV excitation. The present work is completely consistent with their assignments. In comparing the present work with the $(^3He,\alpha)$ experiment of Betts, et al.[33] we also find perfect consistency in the ℓ-values of the 26 states which both experiments see in common, except that the present data indicate mixed ℓ transitions in some cases where the $(^3He,\alpha)$ only indicated a single ℓ-value. Out of the 38 ℓ-assignments from the experiment there are 2 inconsistencies with previous work: an ℓ_p=2 transition was seen in a $(d,n)^{26}$ experiment to a state near the 5244 keV level which is seen with ℓ_n=1+3 in the present experiment, and a state at 4938 which was assigned positive parity in a (p,γ) study is also seen via ℓ_n=1+3 in the present work.

3. Relative spectroscopic factors compared with other experiments.

The ℓ-value assignments listed in Table 4 are quite firm except for the very weak states and weak components of mixed transitions. These determinations are relatively insensitive to the optical model parameters of the DWBA calculations. However, as discussed earlier, the quantitative spectroscopic factors are more parameter dependent, with relative spectroscopic factors being less dependent than absolute values. In connection with a study of the ^{39}K(p,d) rection[46] this parameter dependence of relative spectroscopic factors was investigated with sample results being tabulated in that reference.

The spectroscopic factors given in tables 4 and 5 for the present experiment were calculated using the modified "adiabatic" DWBA prescription described in the data-analysis section of this paper. This parameterization gave the best fits over the range of Q-values covered in this reaction.

The relative spectroscopic factors from the present experiment are compared with those from the (^{3}He,α) reaction[33] in Table 4. In general the agreement is good, with no discrepancies greater than ~20% for states with $C^2S>0.2$. The agreement with the 20 MeV (p,d) experiment of Kroon, et al.[32] is also good, except they extracted a somewhat larger spectroscopic factor for the strong ℓ=2 (T=1) state at 4.7 MeV excitation.

4. Absolute spectroscopic factors.

The comparison of absolute spectroscopic factors between various reactions or between a given reaction and theoretical predictions is a very stringent test of both the reaction theory and nuclear structure theory. Unfortunately, it is relatively easy to incur changes of 30%-50% through parameter variations in the DWBA calculations. As indicated in Figure 7, the "standard" finite-range non-local DWBA prescription yields ℓ=2 spectroscopic factors ~20% smaller and ℓ=0 spectroscopic factors 25-50% larger than the "adiabatic" prescription (when normalized near the primary maxima).

The absolute spectroscopic factors obtained in this work for some of the stronger transitions to states of ^{26}Al are presented in Table 5. The shell model predictions shown there in comparison to them will be discussed in the next two sections.

V. DESCRIPTION OF SHELL MODEL CALCULATIONS

The dual necessities for a viable shell-model description of a nuclear system are that the basis space be adequate to describe the essential degrees of freedom of the system and that the Hamiltonian chosen for the system be "correct". Of course, in neither of these areas is it easy or even possible to establish absolutes. None the less it seems clear that the early attempts[4] to reproduce the features of ^{26}Al in a shell-model space were hampered by both an inadequate basis space (no $d_{3/2}$ excitations, for example) and by a Hamiltonian which failed specifically for the T=0 states of A=26. Since this failure was coincident with the same Hamiltonian successfully accounting for surrounding odd-mass and doubly-even nuclear phenomena, the problem could be viewed primarily as a basis space failure at a more fundamental level. However, other Hamiltonians could produce better results for ^{26}Al at the expense of poorer results for neighboring systems.

A recent calculation by the Glasgow[47] group successfully attacked the conventional basis space problem by computational advances which permitted calculations to be done in the full $d_{5/2}$-$s_{1/2}$-$d_{3/2}$ model space. Their first calculations employed the Kuo two-body Hamiltonian.[48] The consequences of such a choice are illustrated in Fig. 8. It is obvious that a nominally correct basis space alone does very little towards a successful calculation for this 10 particle, doubly-odd system.

The calculations presented here[49] have employed an empirically renormalized two-body interaction[50] (labeled CWP) similar to that described by Preedom and Wildenthal.[51] The present Hamiltonian was adjusted with reference to data in the A=18-24 region and reproduces the spectra of these systems satisfactorily when diagonalized in the full sd-shell space. In light of this, it might be expected that the use of the CWP interaction and the full sd-shell space would successfully account for the ^{26}Al spectra. The use of the full basis space, however, entails quite ardurous computational effort. Consequently we first examined whether a rather mild truncation of the basis space might, when used with the empirically optimized interaction, yield acceptable results. The truncation chosen was to restrict the basis vectors of the $d_{5/2}$-$s_{1/2}$-$d_{3/2}$ space to those which had an occupancy of at least 6 in the $d_{5/2}$ orbit. This served to reduce dimensionalities by about a factor of 3. (The wave function of the ground state of ^{27}Al which was needed for the calculation of the ^{27}Al(p,d)^{26}Al spectroscopic factors, was calculated with a truncation which eliminated all basis states with $d_{5/2}$ occupancy less than 7.) The spectrum resulting from this calculation is shown in Fig. 8, and energies and spectroscopic factors are listed in Table 5.

In order to specifically check the sensitivity of the results calculated in the truncated space to the truncation, the same Hamiltonian was then diagonalized for the T=0 and some T=1 states in the full basis space. These results are also summarized in Fig. 8 and Table 5.

VI. DISCUSSION OF THEORETICAL AND EXPERIMENTAL RESULTS

In the simple $d_{5/2}^n$ model for ^{26}Al only six levels can be populated in neutron pickup from ^{27}Al: J=1, 3 and 5 (T=0) and J=0, 2 and 4 (T=1). The strength by which these states are populated should vary just as (2J+1)(2T+1) when corrections are made for the $C^2(T,T_z)$ factors. The values of these S factors are listed in Table 5 in the column $(d_{5/2})^n$. Inspection of the experimental results shows that indeed there is a strong transition associated with a state of each of the appropriate spin-isospin values and that the qualitative trend of the observed relative strengths roughly follows that of the $(d_{5/2})^n$ model predictions.

The deviations in the data from the simple predictions begin with fact that the lowest 3^+ state is not populated by ℓ=2 ($d_{5/2}$) pickup, but rather by ℓ=0 ($s_{1/2}$). Next, the ℓ=2 strength to J=3, which is smaller than expected, is not concentrated into one state but rather is strongly fragmented. Lastly, three additional positive-parity levels are populated with significant strength and many others weakly.

Before turning to consideration of the degree to which the more complex structure calculations improve the agreement between theoretical and experimental spectroscopic factors, we consider the energy-level spectra. First, it is obvious from Fig. 8 that the spectrum calculated with the Kuo interaction is drastically at variance with experiment. That this results from defects in the interaction seems to follow from the fact that alternate interactions diagonalized in the same basis space yield much better agreement to the data.

The truncated-space calculation is successful in its ordering of the first few levels, but produces much too expanded a spectrum in the first 5 MeV of excitation. The combination of the CWP interaction and the full basis space appropriate for it yields a spectrum which qualitatively reproduces all of the features of the low-excitation energy ^{26}Al spectrum. The results are similar but superior to those obtained[52] with the predecessor "Preedom-Wildenthal" interaction. Hence, as regards level energies at any rate, the inconsistencies between the spectrum of ^{26}Al and its neighbors which appeared in the context of either simpler shell models or inadequate Hamiltonians disappear when the system is treated more fully and carefully. It would seem to follow that there is nothing "anomalous" about ^{26}Al other than that its level structure is much more sensitive to the details of model space and Hamiltonian than is typical of the average nucleus.

Having satisfactorily disposed of the question of the problems of the energy spectrum of ^{26}Al we are still left with the question of the qualitative and quantitative accuracy of the wave functions associated with each level. We confine ourselves here to examination of the pickup spectroscopic factors shown in Table 5. It can be seen from Table 5 that the qualitative deviations from the $(d_{5/2})^n$ predictions which the experimental results show are correctly reproduced by both the "truncated" and full calculations.

Experimentally significant deviations still occur between the measured spectroscopic factors and the theoretical results, however. It must be realized that none of the spectroscopic factor calculations have been done in the full basis space, since the ^{27}Al wave function was not recalculated. Hence both the "full" and "truncated" results of Table 5 are affected by the ^{27}Al truncation. The too-small prediction of ℓ=0 pickup to the first 3^+ state is perhaps one of the consequences. The overall decrease in magnitude of the factors from the truncated to the full calculation can be understood in terms of the smaller average overlap between low-lying state when different truncations are used for daughter and parent states rather than matched truncations.

REFERENCES

1. I. Talmi, Rev. Mod. Phys. 34(1962)704.
2. R. R. Betts, and H. T. Fortune, Phys. Rev. C 7(1973)1257.
3. P. Wasielewski and F. B. Malik, Nucl. Phys. A160(1971)113.
4. B. H. Wildenthal, J. B. McGrory, E. C. Halbert, and P.W.M. Glaudemans, Phys. Lett. 2(1968)692.
5. P. M. Endt and C. van der Leun, Nucl. Phys. A214(1973)1.
6. G. J. Wagner, G. Mairle, U. Schmidt-Rohr, P. Turek, Nucl. Phys. A125(1969)80.
7. B. H. Wildenthal and E. Newman, Phys. Rev. 175(1968)1431.
8. G. A. Bissinger, P. A. Wuin, and P. R. Chugnon, Nucl. Phys. A115(1968)37.
9. G. A. Bissinger, P. A. Quin, and P. R. Chagnon, Nucl. Phys. A132(1969)529.
10. G. A. Bissinger and C. R. Gould, Particles and Nuclei, 3(1972)105.
11. J. W. Noe, D. P. Balamuth, R. R. Betts, H. T. Fortune, and R. W. Zurmuhle, Nucl. Phys. A186(1972)15.
12. O. Hausser, T. K. Alexander, and C. Broude, Can. J. Phys. 46(1968)1035.
13. O. Hausser and N. Anyas-Weiss, Can. J. Phys. 46(1968)2809.
14. C. M. daSilva and J. C. Lisle, Nucl. Phys. A116(1968)452.
15. H. G. Price, A. W. James, P. J. Nolan, J. F. Scharpey-Schafer, P. J. Twin, and D. A. Viggars, Phys. Rev. C6(1972)494.
16. J. F. Sharpey-Schafer, D. C. Bailey, P. E. Carr, A. N. James, P. J. Nolan, and D. A. Viggars, Phys. Rev. Lett. 27(1971)1463.
17. H. G. Price, P. A. Butler, A. N. James, P. J. Nolan, and J. F. Sharpey-Schafer, Phys. Rev. C10(1974)415.
18. J. L. Durell, P. R. Anderson, D. C. Bailey, L. L. Green, M. W. Green, A. N. James, and J. F. Scharpey-Schafer, J. Phys. A5(1972)302.
19. P. Horvat, P. Kump, and B. Povh, Nucl. Phys. 45(1963)341.
20. E. O. de Neijs, M. A. Meyer, J.P.L. Reinecke, and D. Reitmann, Nucl. Phys. A230(1974)490.
21. C. R. Gould, D. R. Tilley, and N. R. Roberson, Phys. Rev. C7(1973)1068.
22. C. E. Moss, C. Detraz, and C. S. Zaidins, Nucl. Phys. A174(1971)408.
23. R. R. Betts, H. T. Fortune, and D. J. Pullen, Bull. Am. Phys. Soc. 16(1971)1433.
24. A. Weidinger, R. H. Siemssen, G. C. Morrison, and B. Zeidman, Nucl. Phys. A108(1968)547.
25. R. H. Siemssen, G. C. Morrison, B. Zeidman, and H. Fuchs Phys. Rev. Lett 16(1966)1050.
26. H. Fuchs, K. Gabisch, P. Kraaz, and G. Roschert, Nucl. Phys. A110(1968)65.
27. R. R. Betts, H. T. Fortune, and D. J. Pullen, Phys. Rev. C6(1972)957.
28. S. Hinds and R. Middleton, Proc. Roy. Soc. (London) 73 (1959)501.
29. D. W. Oliver, K. W. Kemper, and J. D. Fox, Phys. Rev. C8(1973)2144.

30. R. C. Haight, Ph.D. Thesis, Princeton University, 1969.

31. A. S. Anderson and P. R. Bevington, Bull. Am. Phys. Soc. 11(1966)908; A. S. Anderson, Ph.D. Thesis, Stanford University 1968, unpublished.

32. J. Kroon, B. Hird, G. C. Ball, Nucl. Phys. A204(1973)609.

33. R. R. Betts, H. T. Fortune, and D. J. Pullen, Phys. Rev. C8(1973)670.

34. G. J. Wagner, G. Mairle, and U. Schmidt-Rohr, Nucl. Phys. A125(1969)80; M. Arditi, L. Bimbot, H. Doubre, N. Frascaria, J.P. Garron, M. Riou, and D. Royer, Nucl. Phys. A165(1971) 129.

35. B. L. Cohen, Rev. Sci. Instr. 30(1959)415.

36. H. G. Blosser, G. M. Crawley, R. deForest, E. Kashy, and B. H. Wildenthal, Nucl. Inst. and Methods 91(1971)61.

37. E. Kashy, W. Benenson, I. D. Proctor, P. Hauge, and G. Bertsch, Phys. Rev. C7(1973)2251.

38. F. D. Becchetti, Jr. and G. W. Greenlees, Phys. Rev. 182 (1969)1190.

39. J. A. Nolen, Jr., G. Hamilton, E. Kashy, and I. D. Proctor, Nucl. Instr. and Meth. 115(1974)189.

40. A. H. Wapstra and N. B. Gove, Nucl. Data Sec. A 9(1971); N. B. Gove and A. H. Wapstra, Nucl. Data Sec. A 11(1972).

41. Computer code written by P. D. Kunz, University of Colorado.

42. G. R. Satchler, Phys. Rev. C4(1971)1485.

43. R. C. Johnson and P.J.R. Soper, Phys. Rev. C1(1970)976.

44. J. D. Harvey and R. C. Johnson, Phys. Rev. C3(1971)636.

45. F. Hinterberger, G. Mairle, U. Schmid-Rohr, G. J. Wagner, and P. Turek, Nucl. Phys. A111(1968)265.

46. B.H. Wildenthal, J.A. Rice, and B.M. Preedom, Phys. Rev. C 10(1974)2184.

47. B.J. Cole, A. Watt and R.R. Whitehead, Phys. Letters 45B, 429(1973).

48. T.T.S. Kuo, Nucl. Phys. A103, 71(1967).

49. W. Chung, J. Carr, B.H. Wildenthal, D. Larson, and J.B. McGrory, unpublished.

50. W. Chung and B.H. Wildenthal, unpublished.

51. B.M. Preedom and B.H. Wildenthal, Phys. Rev. C6, 1633(1972).

52. B.J. Cole, A. Watt, and R.R. Whitehead, J. of Physics G1, 213(1975).

TABLE 1.--States used in the calibration for the excitation energy analysis.

Reaction	E_x(keV)
$^{27}Al(p,d)$[a]	0[e]
	228.2±0.5
	416.9±0.3
	1057.8±0.4
	2365.2±0.5
	2913.4±0.6
$^{27}Al(p,p)$	0[e]
	843.76±0.03
	1014.46±0.04
	2210.5±0.6
	2734.0±0.9
	3004.2±0.8
$^{16}O(p,d)$	0
$^{16}O(p,p)$	0
$^{12}C(p,d)$[c]	0
	1999.7±0.5[f]
$^{12}C(p,p)$	0
	4439.4±0.3[f]
$^{28}Si(p,d)$[d]	0

a Ref. 40, Q_o = -10833.3±0.9 keV.
b Ref. 39, Q_o = -13439.3±0.8 keV.
c Ref. 40, Q_o = -16497.2±1.1 keV.
d Ref. 40, Q_o = -14952.8±1.8 keV.
e Ref. 5.
f Ref. 39.

TABLE 2.--Accurate excitation energy assignments in ^{26}Al.

Previous γ-work[a]	(p,γ)[b]	(^{3}He,pγ)[c]	(p,d)[d]	Weighted average[e]
0.0			0.0[f]	0.0
228.2±0.5			228[f]	228.2±0.5
416.9±0.3	416.7±0.5		417[f]	416.8±0.3
1057.8±0.4			1058	1057.8±0.4
1759.3±0.6			1759±1	1759.2±0.5
1850.6±0.8			1850±1	1850.4±0.6
2068.7±0.3				2068.7±0.3
2069.5±0.3			2069±1[g]	2069.5±0.3
2071.7±0.7				2071.7±0.7
2365.2±0.5	2364.9±0.7		2365[f]	2365.1±0.4
2545.3±0.5			2545±1	2545.2±0.4
2660.8±0.4			2663±2	2660.9±0.4
2739.3±1.2	2738.9±1.0		2740±1	2739.4±0.6
2913.4±0.6	2912.7±0.7		2913[f]	2913.1±0.5
3074. ±5.	3073.1±1.4		3073±1	3073.1±0.8
3159.4±1.0	3160.0±1.2		3159±1	3159.4±0.6
3403.5±0.5	3402.8±0.8		3402±1	3403.1±0.4
3507.5±0.5	3506. ±4.		3507±1	3507.4±0.4
	3595.5±1.6	3598 3	3596±1	3596.0±0.8
-	3672.5±1.6		3675±2	3673.5±1.2
	3680.7±1.6	3680 1	3681±1	3680.5±0.6
	3723.0±1.6	3720 1	3723±1	3722.2±0.6
(3745.4±1.2)[i]	3749.8±1.8	3750 1	3751±1[h]	3749.9±0.9
	3753.1±1.0	3754 1		3753.6±0.7
			3923±2	3923 ±2
	3962.5±1.2	3962 1	3963±1	3962.5±0.6
		3979 1	3976±2	3978.4±0.9
	4192.0±2.0		4191±1	4191.2±0.9
	4205.0±2.0		4206±1	4205.8±0.9
	4349.0±2.2		4349±2	4349.0±1.5
	4430.0±1.3		4430±2	4430.0±1.1
	4479.4±1.0		-	4479.4±1.0
	4548.6±2.2		4546±1	4546.4±0.9
	4598.7±1.6		4598±1	4598.2±0.8
	4622.0±1.5		-	4622.0±1.5
	4705.6±1.3		4704±1	4704.6±0.8
	4772.6±2.2		4771±2	4771.7±1.5
	4938.0±1.0		4939±2	4938.2±0.9
	4952.4±1.4		4950±2	4951.6±1.1
	-		5006±2	5006 ±2
	5131.4±0.9		(5030±2)[j]	5131.4±0.9
	5141.7±2.0		5139±2	5140.3±1.4
	-		5194±5	5194 ±5
	5244.5±2.0		5244±3	5244.3±1.7
	5394.0±1.0		5392±2	5393.6±0.9
	5456.6±2.5		5453±2	5454.4±1.6
	-		5491±2	5491 ±2

TABLE 3.--Optical model parameters used in DWBA calculations with the program DWUCK for $^{27}Al(p,d)^{26}Al$ at 35 MeV proton energy.

Channel	V (MeV)	r_o (F)	a (F)	W (MeV)	r_I (F)	a_I (F)	W_D (MeV)	V_{so} (MeV)	r_{so} (MeV)	a_{so} (F)
proton[a]	-45.42	1.17	0.75	-5.0	1.32	0.54	13.97	-24.8	1.01	0.75
deuteron(A)[b]	-99.05	1.17	0.78	-1.09	1.35	0.58	69.8	-12.4	1.01	0.75
deuteron(B)[c]	-77.5	1.25	0.739	0.0	1.25	0.735	52	-12.0	1.25	0.739
neutron	V[d]	1.24	.65					λ =25		

a Becchetti-Greenlees parameters.[38]

b Adiabatic potential with Becchetti-Greenlees parameters; calculations done in local, zero-range approximation.

c Hinterberger paramters.[46]; calculations done in finite-range, non-local approximation with non locality parameters of 0.85 and 0.54 for the proton and deuteron channels, respectively, and a finite range parameter of 0.67.

d Well depth adjusted to fit separation energy.

TABLE 2.--Continued.

Previous γ-work[a]	$(p,\gamma)^b$	$(^3He,p\gamma)^c$	$(p,d)^d$	Weighted average[e]
	5514.2±1.8		5509±3	5512.8±1.5
	5544 ±3		5541±3	5542.5±2.1
	-		5566±3	5566 ±3
	5583.0±1.5		--	5583.0±1.5
	-		5595±2	5595 ±2
	5674.3±1.0		5671±3	5674.0±1.0
	5691.7±1.4		5688±3	5690.5±1.3
	5725.9±2.5		5723±3	5724.7±1.9
	(5848.8±2.5)[j]		5845±3[k]	5845 ±3
	5913.5±1.0			5913.5±1.0
	6082.6±2.2			6082.6±2.2

a Endt and van der Leun, Reference 5.

b de Neijs, Meyer, Reinecke, and Reitmann, Reference 20.

c Bissinger and Gould, Reference 10.

d Present work.

e Excitation energies and uncertainties weighted according to $1./\sigma^2$.

f Calibration lines for present work, not included in weighted averages.

g Unresolved 3 keV triplet, not included in weighted averages.

h Unresolved 4 keV doublet, dominated by the lower member, but not included in the weighted averages.

i Seen in Reference 8, but omitted from present weighted average due to possible unresolved components.

j Uncertain level, not included in weighted average.

k Highest level scanned in present work.

TABLE 4.--Spin assignments and relative spectroscopic factors for states of ^{26}Al.

E_x (keV)	J γ-ray assignments[a]	J Transfer Reactions[b]	ℓ_n	C^2S (^{3}He,α)[c]	C^2S (p,d)[d]
0	5^+		2	1.00	1.00
228	0^+		2	0.14	0.14
417	3^+		2	---	.05
			0	0.12	0.15
1058	1^+		2	0.31	0.31
1759	2^+		2	0.02	0.02
			0	0.01	0.023
1850	1^+		2	(0.02)	0.016
2069	4^+				
2070	2^+		2	0.50	0.52
2072	1^+		0	---	-.016
2365	3^+		2	0.26	0.23
			0	---	.018
2545	3^+		2	0.30	0.30
2661	$(2,3)^+$		-	---	---
2739	1^+		-	---	---
2913	2^+		2	---	0.025
			0	---	.001
3073	$(2,3^+)^e$	$(2,3)^{+f}$	-	---	---
3159	2^+		2	0.10	0.10
			0		.003
3403	5^+		2	0.08	0.09
3507	6^+		(4)		(0.04)
3596	$(2,3)^+$		2	0.006	0.013
			0	0.004	0.003
3674	$(3,4^+)^e$		2	0.14	0.16
3681	$\leq 4^e$		0	0.01	0.01
3722	1^+		2	---	0.016
3750	$(2)^+$		2	0.016	0.028
3754	0^{+g}		0	0.02	0.02
3923	$(7,5)^{+m}$		(4)		(0.04)
3963	3^e	3^+	2	0.08	0.08
			0	0.03_h	0.05_h
3978	$(0,1)_-$		-	----[i]	----
4191	$(2,3)^+$		2	0.03[i]	0.009
			0	0.002	0.004
4206	$\geq 3^e$	$\geq 3^+$	2		0.016
4349		$(0-5)^+$	2	0.02	0.03
4430		$(1-4)^-$	3	---	0.05
			1	0.02	0.02

Table 4 cont'd.

E_x (keV)	J γ-ray assignments[a]	J Transfer Reactions[b]	ℓ_n	C^2S (^{3}He,α)[c]	C^2S (p,d)[d]
4479			-		
4546		$(2,3)^+$	2	0.06	0.05
			0	0.02	0.02
4598		$(2,3)^+$	2	0.02	0.02
			0	0.02	0.03
4622			-	---	---
4705	$(3,4)^e$	4^+n	2	0.86	0.71
4772	$+^e$	$(0-5)^+$	2	---	0.015
4938	$(1,2)^{+e}$		3[j]	---	0.02
			1[j]	---	0.02
4952		$(0-5)^+$	2	[illegible]	[illegible]
5006		$(0-5)^+$	2	---	[illegible]
5131			-		
5140		$(2,3)^+$	0	0.06	0.03
5194			-	---	
5244		$(1-4)^-$	3[k]	---	0.005
			1[k]	---	0.007
5394		$(-)^1$	-	---	
5454		$(-)^1$		---	
5491		$(2,3)^+$	2	0.03	0.007
			0	0.01	0.014
5513		(1^--6^-)	(3)		(0.003)
5543		$(2,3)^+$	2	---	0.01
			0	---	0.007
5566		(1^--4^-)	(3)	---	(0.005)
			(1)	---	(0.003)
5583			-	---	
5595		$(1-4)^-$	3	---	0.02
			1	0.17	0.12
5674			-		
5691		(0^+-5^+)	(2)		
5725		4^+n	2	0.18	0.12
5845			-		

a From Endt and van der Leun,[5] except where indicated otherwise.

b Additional constraints on J provided by particle transfer reaction

c From Betts, Fortune, and Puller[27]; C^2S normalized to 1.00 for the ground state.

d Present results with C^2S normalized to 1.00 for the ground state. Comparison with previous (p,d) work[32] at lower energy is given in the text.

e From de Neijs, Meyer, Reinecke, and Reitmann.[20]

f Seen via L=2 in (,d)[29].

g From Bissinger and Gould.[10]

h Unresolved from 3963 keV level in (^{3}He,), but shown to be very wea in the (p,d) experiment.

i Includes contributions from both 4191 and 4206 keV levels.

Table 5. Experimental and theoretical energies and spectroscopic factors for some states of ^{26}Al. The theoretical energies for the 5^+ ground state are the nuclear binding energies relative to ^{16}O.

^{26}Al states (J,T)	Excitation Energies (MeV) CWP trun.	CWP full	exp.	100 x spectroscopic factor S(j) CWP trun. 1/2	3/2	5/2	CWP full 1/2	3/2	5/2	$(d_{5/2})^n$ 5/2	exp ℓ=0	ℓ=2
$1,0)_1$	1.56	1.20	1.05		1.3	41.		0.7	33.	50		43
2	4.33	2.23	1.89		0.5	0.3		0.8	2.2			2
3	4.69	2.57	2.07		0.3	0.1		0.2	0.1			
4	5.12	3.13	2.74		0.7	0.3		0.2	0.5			
5	5.61	4.29	3.72									
6	7.44	5.88										
$2,0)_1$	2.93	2.19	1.76	1.3	1.0	0.2	1.1	0.6	0.2	0	3	3
2	4.93	2.94	2.07	0.2	1.3	0.0	0.0	0.2	0.0			
3	5.26	3.46		0.4	0.6	0.0	0.1	0.9	0.1			
4	6.09	40.6		0.7	0.2	0.0	0.3	0.4	0.1			
$3,0)_1$	1.97	0.83	0.41	7.5	0.7	0.8	4.8	0.6	0.2	117	21	7
2	2.69	2.31	2.36	1.6	1.4	73.	1.1	1.4	51.		3	32
3	3.76	2.92	2.54	0.1	0.7	7.7	0.1	0.7	0.1		1	42
4	4.68	3.51		1.0	3.6	1.8	0.4	0.0	0.2			
5	5.12	3.88							9.4			
6	5.54	4.14							11.4			
$4,0)_1$	3.09	2.16	2.07							0		
2	4.92	4.15										
3	6.01	4.39										
$5,0)_1$	(105.72)	(106.45)	0.00			136.			123.	183		140
2	4.31	3.57	3.40			3.3			6.4			13
3	6.62	5.38				3.6			0.6			
4		5.85				12.			5.7			
$0,1)_1$	0.51	0.12	0.22			46.			40.	50		60
2	6.27	4.21	3.75			0.2			2.6			
3	7.87	5.36				0.1			1.2			

Table 4 cont'd.

j Inconsistent with positive parity assignment in $(p,\gamma)^{20}$.

k Inconsistent with an ℓ_p=2 transition seen in $(d,n)^{26}$.

l Two transitions with ℓ_p=1 were seen in this region via $(d,n)^{26}$.

m Present observation of uncertain ℓ_n=3 with C^2S=0.3 is inconsistent with $(^3He,\sigma)^{27}$.

n Ref. 17 - Spin assignment based on this state being T=1 analog of state is ^{26}Mg via comparison of spectroscopic factors.

Table 5--cont.

2,1)$_1$	2.67	2.18	2.07	1.7	0.1	180.	290	6	220
	4.56			0.8	0.9	2.8		3	42
2	6.08			8.6	3.8	4.9			
3	7.10			0.6	0.1	0.2			
4									
4,1)$_1$	4.68		4.71		3.0	308.	450		297
	6.14		5.72		0.1	1.9			51
2	7.02				0.0	12.			
3									

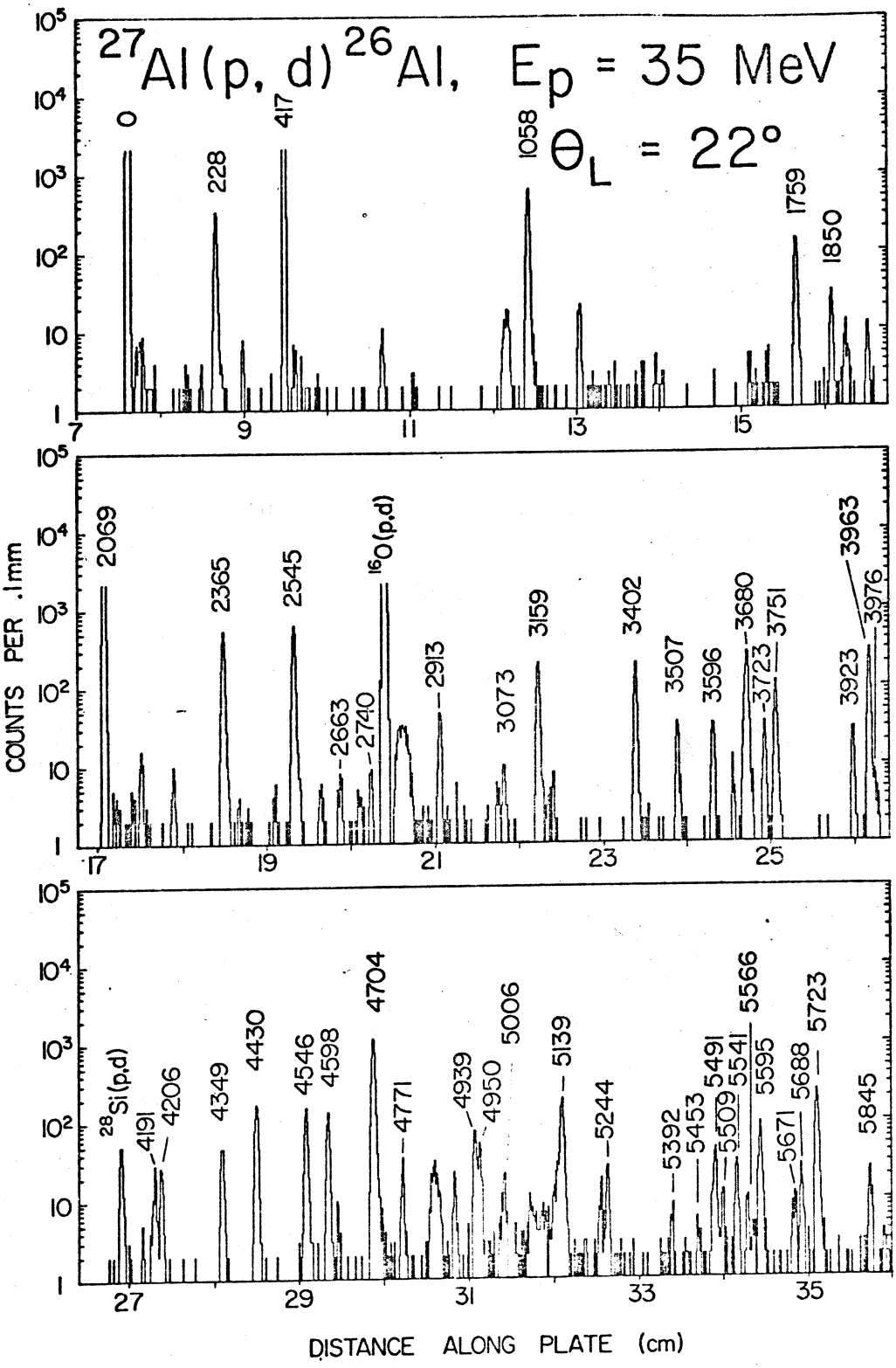

Figure 1. Spectrum of deuterons from the ^{27}Al(p,d) reaction scanned from the nuclear emulsions in 0.1 mm steps. The excitation energies of the states in ^{26}Al are indicated in keV. The unlabeled peaks have been identified via Q-values and kinematic shifts as known states arising from (p,d) reactions on ^{13}C, ^{14}N, ^{23}Na, ^{28}Si, and ^{31}P, as well as (p,t) reactions on ^{13}C, ^{16}O, and ^{27}Al.

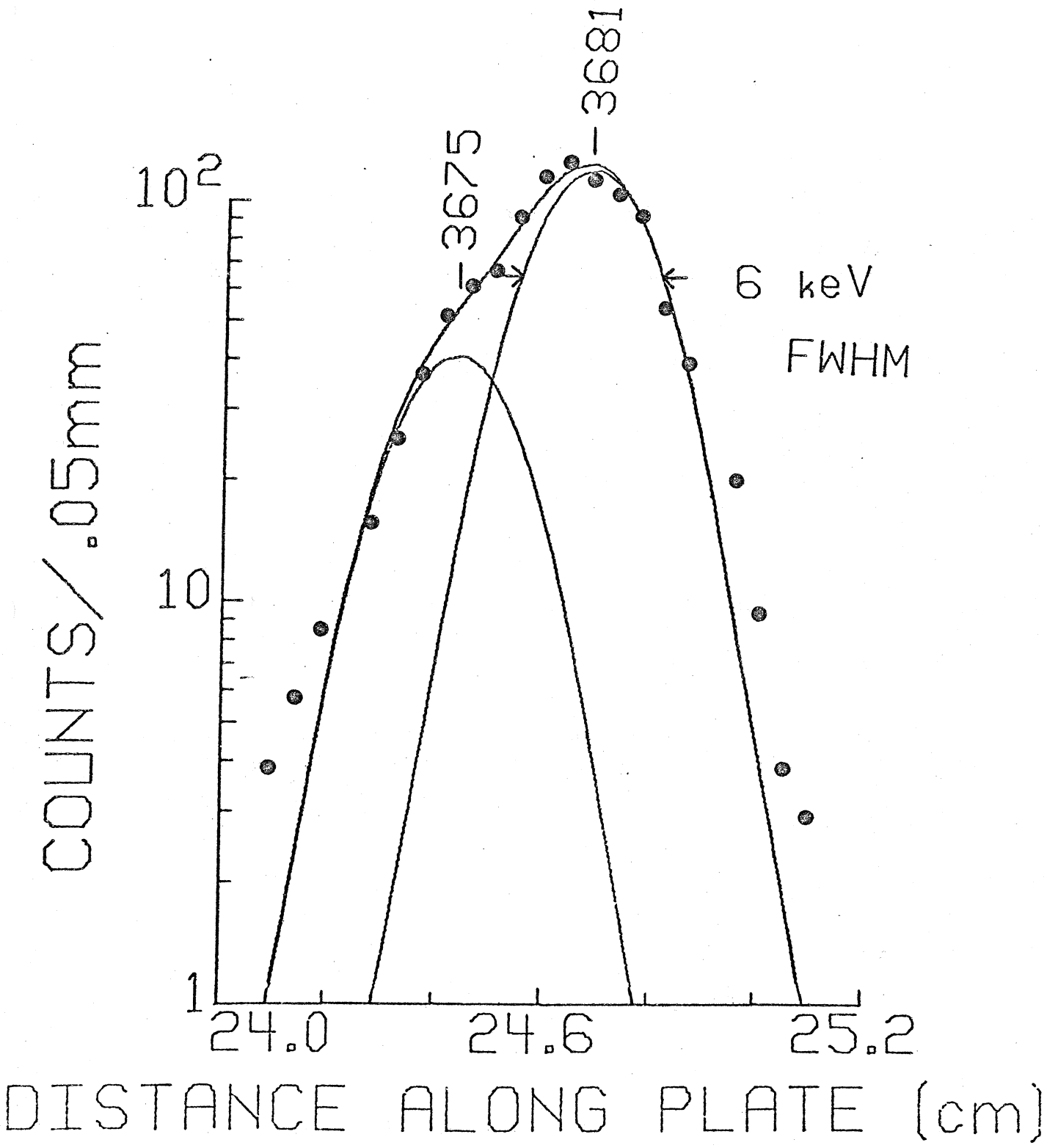

Figure 2. A scan of the 3675, 3681 keV doublet done in 0.05 mm steps and fit with a Gaussean plus exponential tails to determine the peak separation and relative yields.

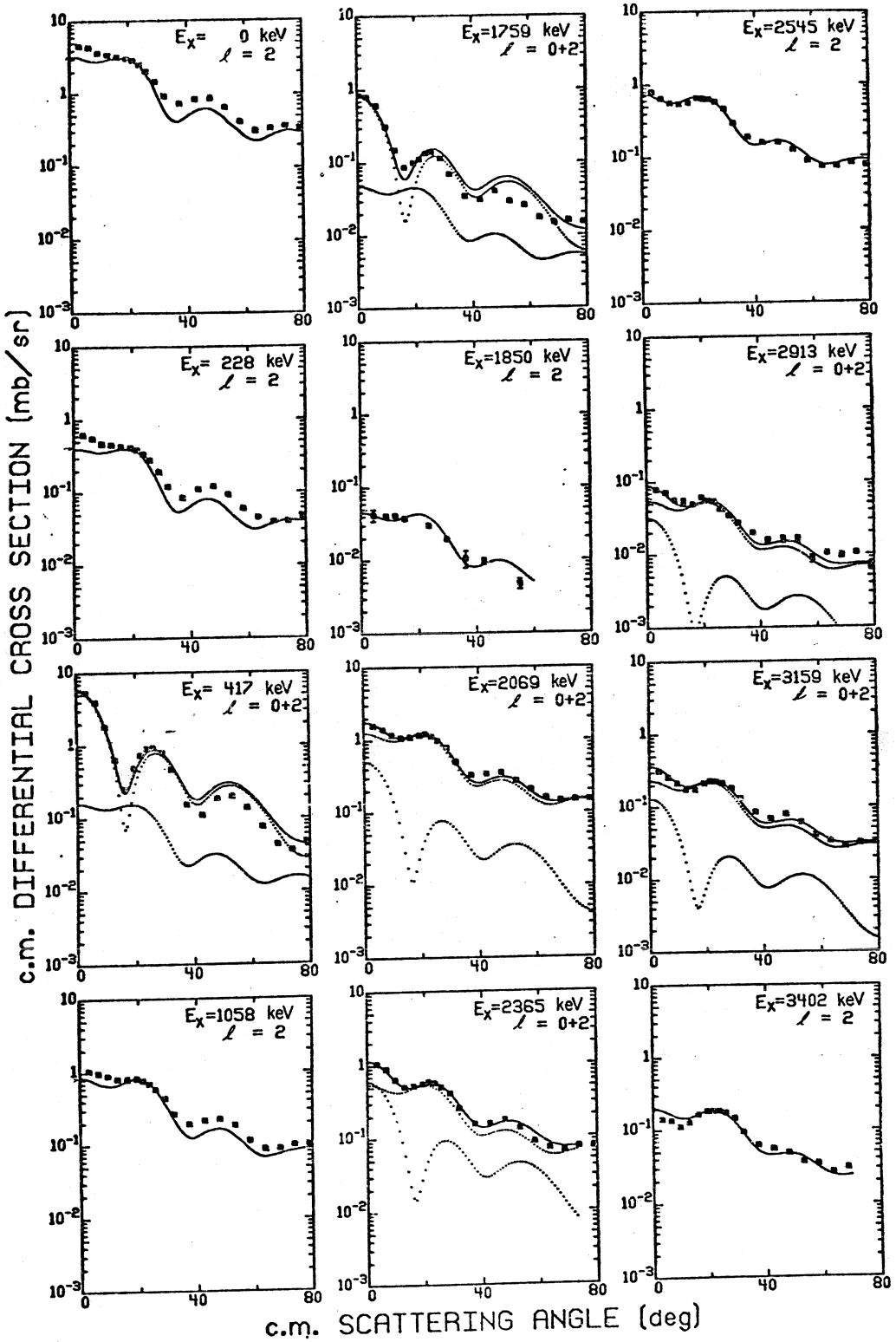

Figure 3. Angular distribution of the ^{27}Al(p,d) transitions to states of ^{26}Al. The curves are DWBA calculations described in the text with ℓ-values indicated in each case. For the mixed-ℓ transitions the dotted curves indicate the relative contribution of the separate ℓ-values.

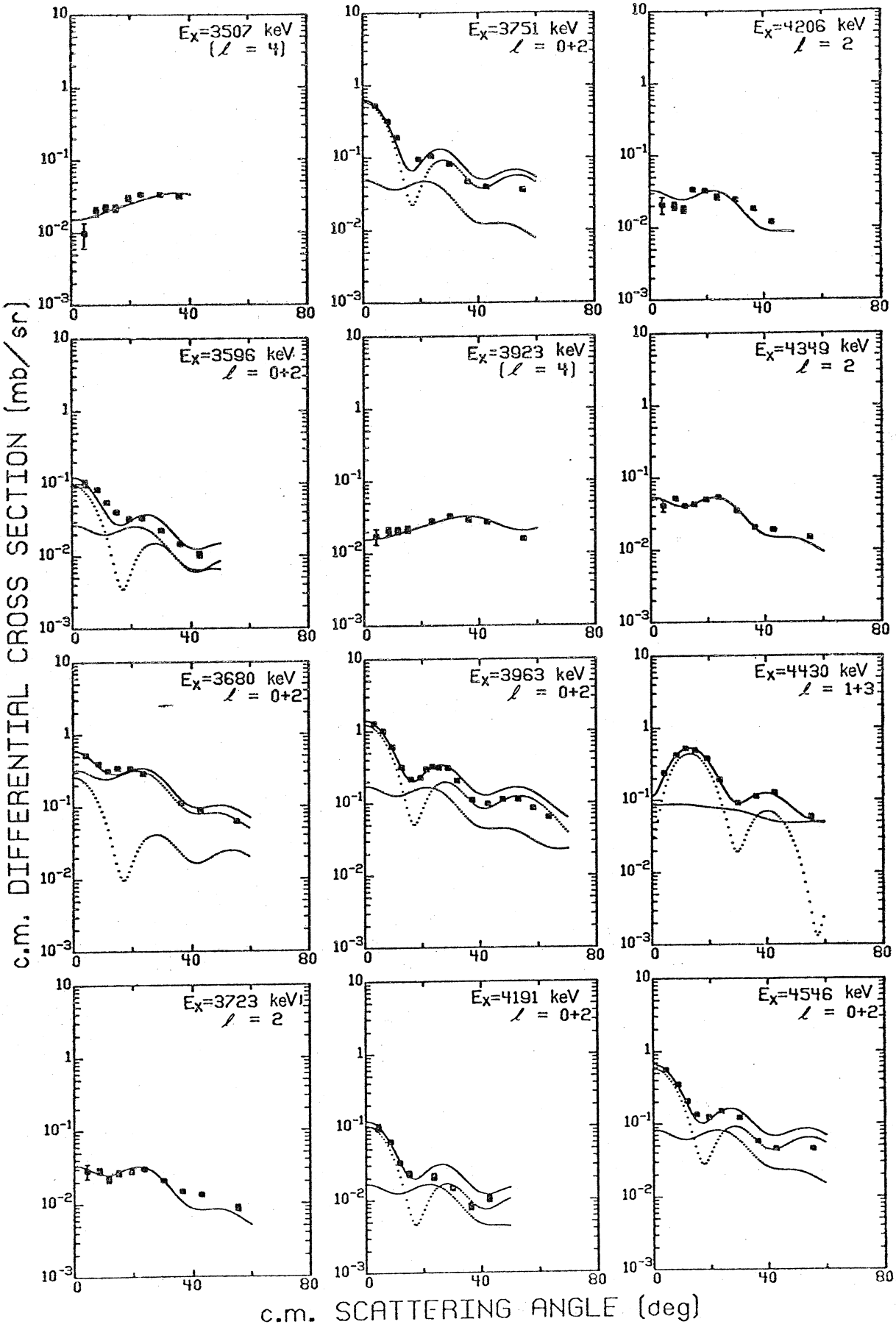

Figure 4-6. Same as Figure 3.

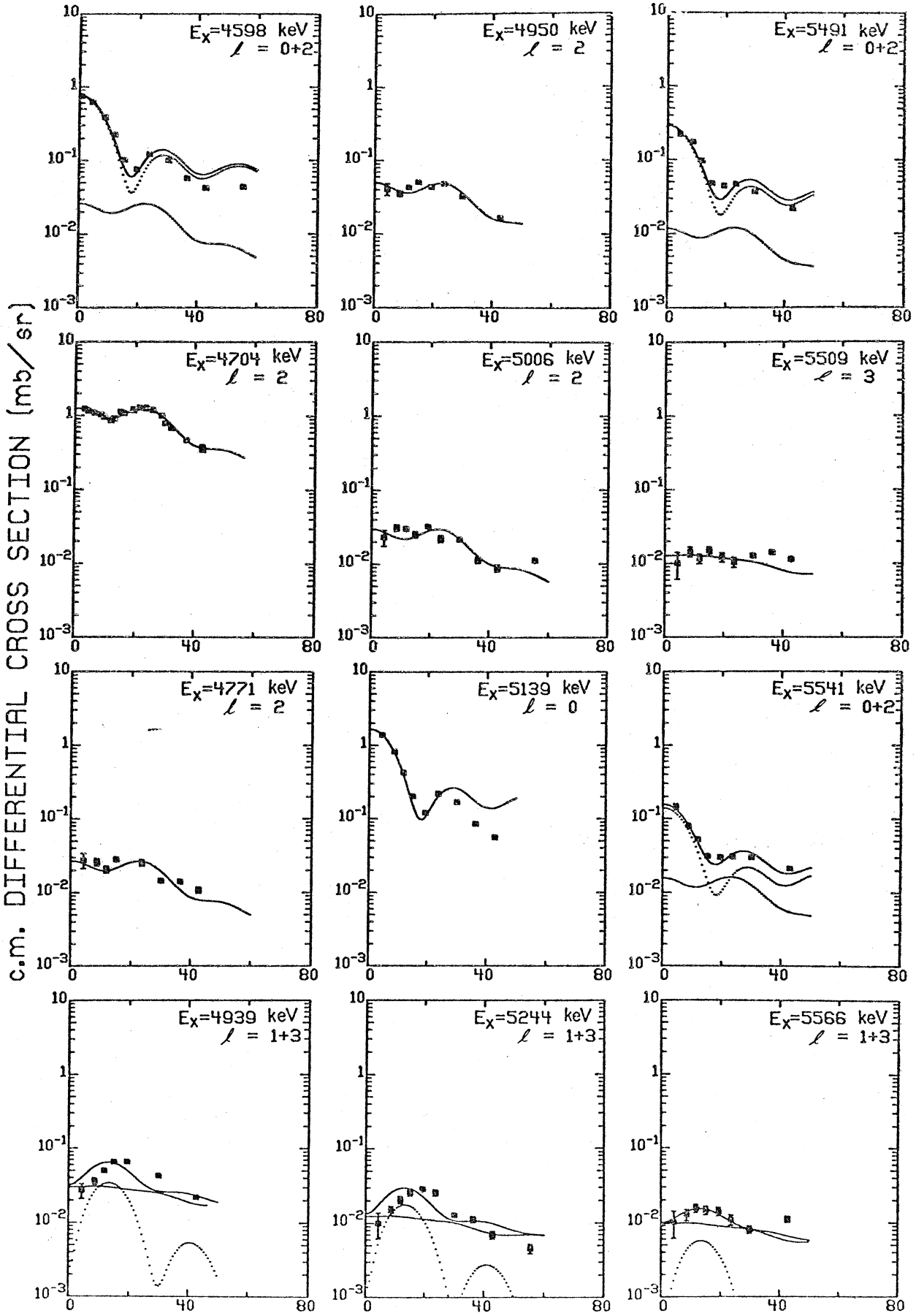
Ex=4598 keV
ℓ = 0+2
Ex=4950 keV
ℓ = 2
Ex=5491 keV
ℓ = 0+2
Ex=4704 keV
ℓ = 2
Ex=5006 keV
ℓ = 2
Ex=5509 keV
ℓ = 3
Ex=4771 keV
ℓ = 2
Ex=5139 keV
ℓ = 0
Ex=5541 keV
ℓ = 0+2
Ex=4939 keV
ℓ = 1+3
Ex=5244 keV
ℓ = 1+3
Ex=5566 keV
ℓ = 1+3
c.m. DIFFERENTIAL CROSS SECTION (mb/sr)
c.m. SCATTERING ANGLE (deg)

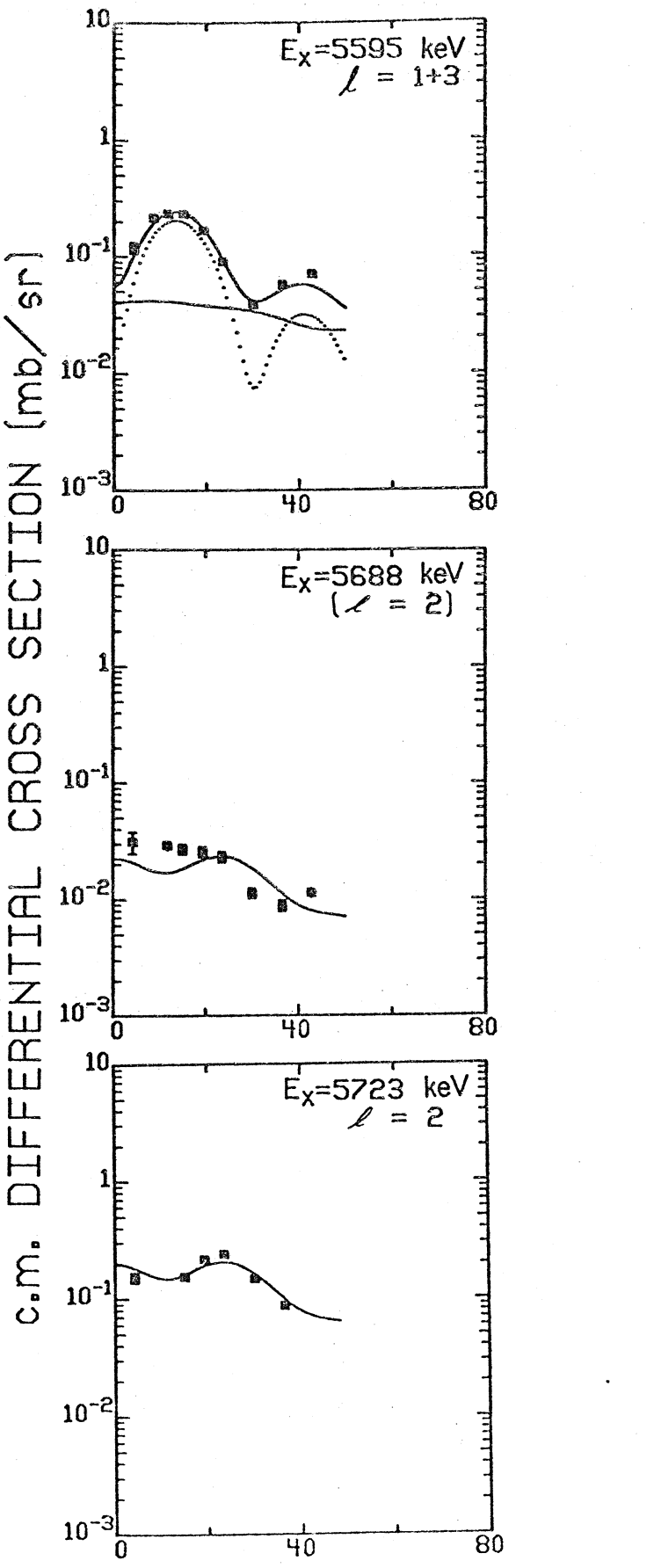
E_x=5595 keV
ℓ = 1+3
E_x=5688 keV
(ℓ = 2)
E_x=5723 keV
ℓ = 2
c.m. DIFFERENTIAL CROSS SECTION (mb/sr)
c.m. SCATTERING ANGLE (deg)
10
1
10^{-1}
10^{-2}
10^{-3}
0
40
80

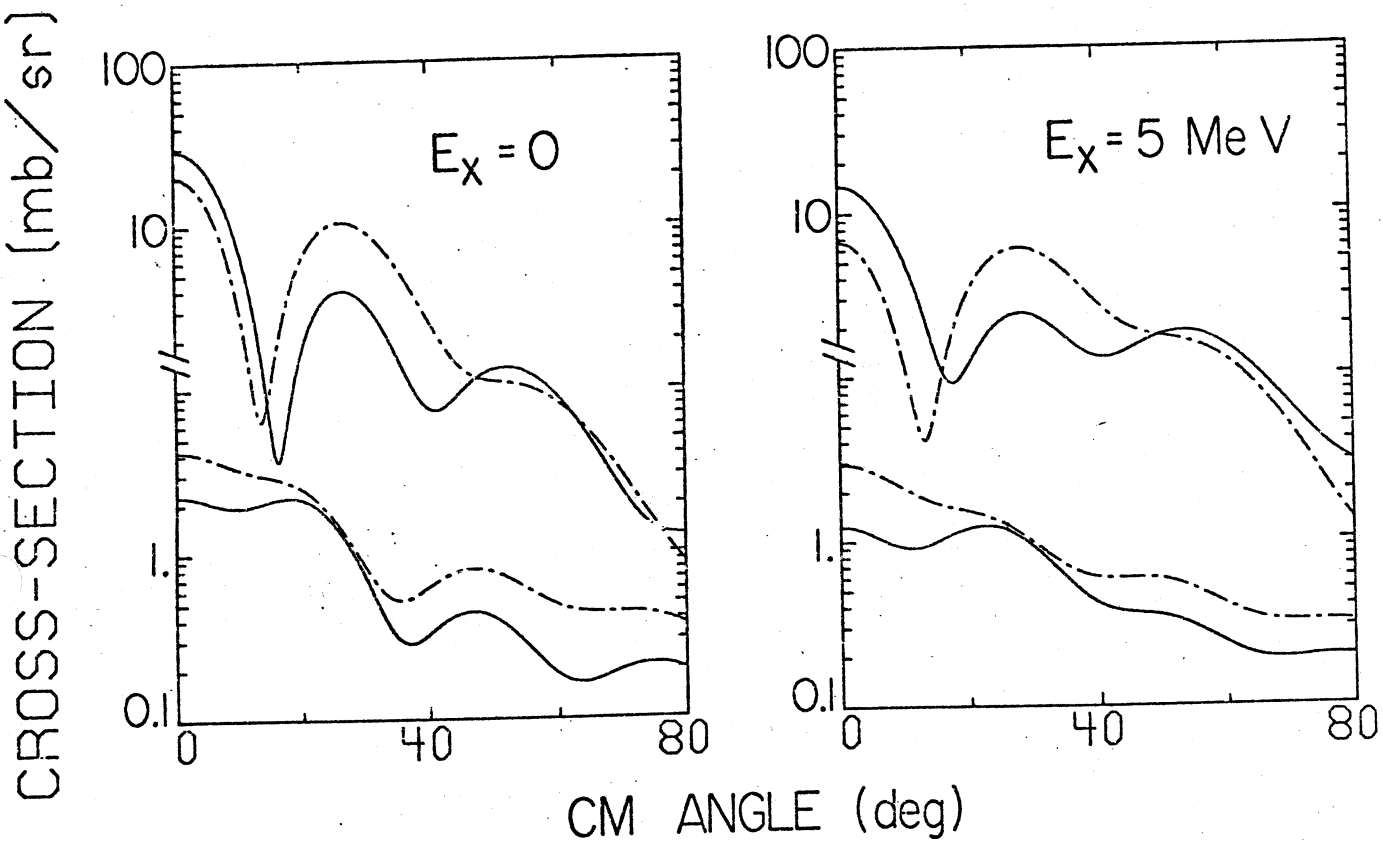

Figure 7. Sample DWBA calculations for ^{27}Al(p,d) transitions of unit spectroscopic factor to indicate parameter dependence and Q-dependence. The upper two curves in each case are for $1/2^+$ transitions and the lower ones are for $5/2^+$ transitions. The solid curves are "adiabatic" calculations and the broken ones result from Hinterberger parameters.

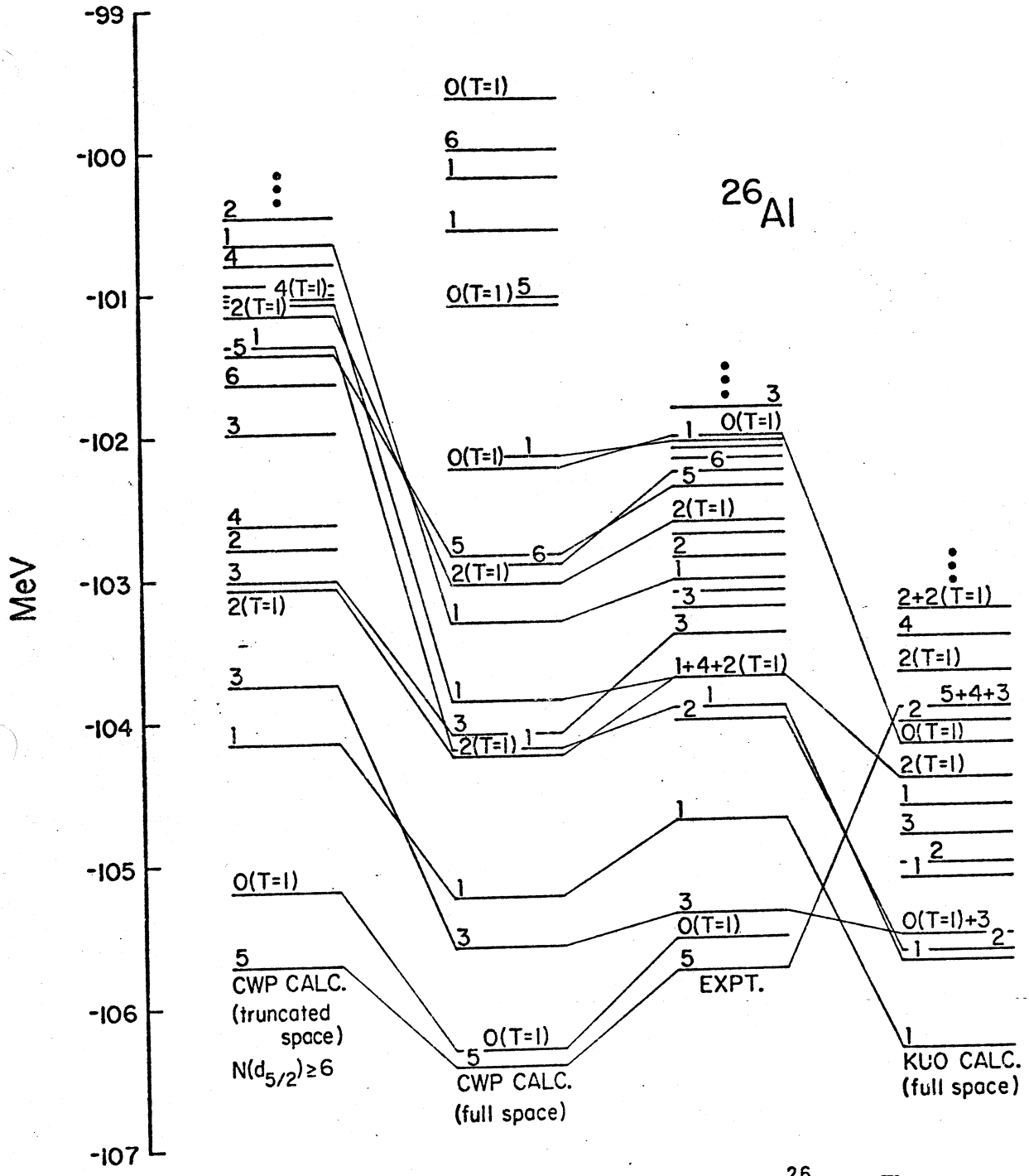

Figure 8. Experimental and theoretical spectra of ^{26}Al. The "CWP truncated" column indicates results obtained in the truncated space with an empirically optimized Hamiltonian, the "CWP full" column shows results with the same Hamiltonian in the full sd-shell space, and the "Kuo" column shows results of diagonalizing Kuo's matrix elements in the full space. The binding energy scale for the Kuo results has been arbitrarily shifted to match up the 0^+,T=1 states.

CORRECTED TABLES

TABLE 2.--Accurate excitation energy assignments in ^{26}Al.

Previous γ-work[a]	(p,γ)[b]	(^{3}He,pγ)[c]	(p,d)[d]	Weighted average[e]
0			0[f]	0
228.2±0.5			228.2[f]	228.2±0.5
416.9±0.3	416.7±0.5		416.8[f]	416.8±0.3
1057.8±0.4			1057.8[f]	1057.8±0.4
1759.3±0.6			1758.5±1.0	1759.1±0.5
1850.6±0.8			1849.9±1.0	1850.3±0.6
2068.7±0.3				2068.7±0.3
2069.5±0.3			2069.2±1.0[g]	2069.5±0.3
2071.7±0.7				2071.7±0.7
2365.2±0.5	2364.9±0.7		2365.1[f]	2365.1±0.4
2545.3±0.5			2544.7±1.3	2545.2±0.5
2660.8±0.4			2662.5±2.0	2660.9±0.4
2739.3±1.2	2738.9±1.0		2740.1±1.4	2739.3±0.7
2913.4±0.6	2912.7±0.7		2913.1[f]	2913.1±0.5
3074 ±5	3073.1±1.4		3072.8±1.5	3073.0±1.0
3159.4±1.0	3160.0±1.2		3159.3±1.6	3159.6±0.7
3403.5±0.5	3402.8±0.8		3402.4±1.7	3403.3±0.4
3507.5±0.5	3506 ±4		3507.4±1.7	3507.5±0.5
	3595.5±1.6	3598±3	3595.9±1.8	3596.0±1.1
	3672.5±1.6		3675.0±2.0	3673.5±1.2
	3680.7±1.6	3680±1	3681.0±2.0	3680.3±0.8
	3723.0±1.6	3720±1	3723.4±1.9	3721.3±0.8
(3745.4±1.2)[i]	3749.8±1.8	3750±1	3751.3±1.9[h]	3750.0±0.9
	3753.1±1.0	3754±1		3753.6±0.7
			3922.5±1.9	3922.5±1.9
	3962.5±1.2	3962±1	3963.1±2.0	3962.3±0.7
		3979±1	3976.0±3.0	3978.7±0.9
	4192.0±2.0		4190.5±2.1	4191.3±1.4
	4205.0±2.0		4205.5±2.1	4205.2±1.4
	4349.0±2.2		4348.5±2.2	4348.8±1.6
	4430.0±1.3		4429.5±2.2	4429.9±1.1
	4479.4±1.0		—	4479.4±1.0
	4548.6±2.2		4545.7±2.2	4547.2±1.6
	4598.7±1.6		4597.5±2.3	4598.3±1.3
	4622.0±1.5		—	4622.0±1.5
	4705.6±1.3		4703.5±2.3	4705.1±1.1
	4772.6±2.2		4770.5±2.4	4771.6±1.6
	4938.0±1.0		4938.5±2.4	4938.1±0.9
	4952.4±1.4		4949.5±2.5	4951.7±1.2
	-		5005.5±2.5	5005.5±2.5
	5131.4±0.9		(5030±2)[d]	5131.4±0.9
	5141.7±2.0		5138.7±2.6	5140.6±1.6
	-		5194± 5	5194± 5
	5244.5±2.0		5243.5±2.6	5244.1±1.6
	5394.0±1.0		5391.7±2.7	5393.7±0.9
	5456.6±2.5		5453.0±2.7	5454.9±1.8
	-		5491.3±2.7	5491.3±2.7

TABLE 2.--Continued.

Previous γ-work[a]	$(p,\gamma)^b$	$(^3He,p\gamma)^c$	$(p,d)^d$	Weighted average[e]
	5514.2±1.8		5509.2±2.8	5512.7±1.5
	5544 ±3		5541.0±2.8	5542.4±2.0
	-		5566.4±2.8	5566.4±2.8
	5583.0±1.5		—	5583.0±1.5
	-		5595.3±2.8	5595.3±2.8
	5674.3±1.0		5671.1±2.8	5673.9±0.9
	5691.7±1.4		5688.0±2.9	5691.0±1.3
	5725.9±2.5		5723.1±2.9	5724.7±1.9
	(5848.8±2.5)[j]		5845.4±2.9[k]	5845.4±2.9
	5913.5±1.0			5913.5±1.0
	6082.6±2.2			6082.6±2.2

[a]Endt and van der Leun, Reference 5.

[b]de Neijs, Meyer, Reinecke, and Reitmann, Reference 20.

[c]Bissinger and Gould, Reference 10.

[d]Present work.

[e]Excitation energies and uncertainties weighted according to $1/\sigma^2$.

[f]Calibration lines for present work, not included in weighted averages.

[g]Unresolved 3 keV triplet, not included in weighted averages.

[h]Unresolved 4 keV doublet, dominated by the lower member, but not included in the weighted averages.

[i]Seen in Reference 8, but omitted from present weighted average due to possible unresolved components.

[j]Uncertain level, not included in weighted average.

[k]Highest level scanned in present work.

TABLE 4.--Spin assignments and relative spectroscopic factors for states of ^{26}Al.

E_x (keV)	J Previous assignments[a]	J Transfer Reactions[b]	ℓ_n	C^2S ($^3He,\alpha$)[c]	C^2S (p,d)[d]
0	5^+		2	1.00	1.00
228	0^+		2	0.14	0.14
417	3^+		2	---[o]	.05
			0	0.12	0.15
1058	1^+		2	0.31	0.31
1759	2^+		2	0.02	0.02
			0	0.01	0.023
1850	1^+		2	(0.02)	0.016
2069	4^+		2	0.50	0.52
2070	2^+		0	---[o]	$\leq$.016
2072	1^+				
2365	3^+		2	0.26	0.23
			0	---[o]	.018
2545	3^+		2	0.30	0.30
2661	$(2,3)^+$		-	---	---
2739	1^+		-	---	---
2913	2^+		2	---[o]	0.025
			0	---[o]	.001
3073	$(2,3^+)^e$	$(2,3)^+$[f]	-	---	---
3159	2^+		2	0.10	0.10
			0	---[o]	.003
3403	5^+		2	0.08	0.09
3507	6^+		(4)		(0.04)
3596	$(2,3)^+$		2	0.006	0.013
			0	0.004	0.003
3674	$(3,4^+)^e$		2	0.14	0.16
3681	$\leq 4^e$		0	0.01	0.01
3722	1^+		2	---[o]	0.016
3750	$(2)^+$		2	0.016	0.028
3754	0^+[g]		0	0.02	0.02
3923	$(7,5)^+$[m]		(4)		(0.04)
3963	3^e	3^+	2	0.08	0.08
			0	0.03[h]	0.05[h]
3978	$(0,1)$		-	----[i]	----
4191	$(2,3)^+$		2	0.03	0.009
			0	0.002	0.004
4206	$\geq 3^e$	$(3-5)^+$	2		0.016
4349		$(0-5)^+$	2	0.02	0.03
4430		$(1-4)^-$	3	---[o]	0.05
			1	0.02	0.02

Table 4 cont'd.

E_x (keV)	J γ-ray assignments[a]	J Transfer Reactions[b]	ℓ_n	C^2S ($^3He,\alpha$)[c]	C^2S (p,d)[d]
4479			-		
4546		$(2,3)^+$	2	0.06	0.05
			0	0.02	0.02
4598		$(2,3)^+$	2	0.02	0.02
			0	0.02	0.03
4622			-	---	---
4705	$(3,4)^e$	$(2-4)^{+n}$	2	0.86	0.71
4772	$^{+e}$	$(0-5)^+$	2	---[o]	0.015
4938	$(1,2)^{+e}$		3[j]	---[o]	0.02
			1[j]	---[o]	0.02
4952		$(0-5)^+$	2	0.06	0.03
5006		$(0-5)^+$	2	---[o]	0.02
5131			-		
5140		$(2,3)^+$	0	0.06	0.03
5194			-	---	---
5244		$(1-4)^-$	3[k]	---[o]	0.005
			1[k]	---[o]	0.007
5394		$(-)^1$	-	---	---
5454		$(-)^1$		---	---
5491		$(2,3)^+$	2	0.03	0.007
			0	0.01	0.014
5513		(1^--6^-)	(3)	---	(0.003)
5543		$(2,3)^+$	2	---[o]	0.01
			0	---[o]	0.007
5566		(1^--4^-)	(3)	---	(0.005)
			(1)	---	(0.003)
5583			-	---	---
5595		$(1-4)^-$	3	---[o]	0.02
			1	0.17	0.12
5674			-		
5691		(0^+-5^+)	(2)		
5725		4^{+n}	2	0.18	0.12
5845			-		

a From Endt and van der Leun,[5] except where indicated otherwise.

b Additional constraints on J^π provided by particle transfer reactions, from references 24, 26, 27, 29, 32, 33 and present work.

c From Betts, Fortune, and Pullen[33]: C^2S normalized to 1.00 for the ground state.

d Present results with C^2S normalized to 1.00 for the ground state. Comparison with previous (p,d) work[32] at lower energy is given in the text.

e From de Neijs, Meyer, Reinecke, and Reitmann.[20]

f Seen via L=2 in (α,d)[29].

g From Bissinger and Gould.[10]

h Unresolved from 3963 keV level in ($^3He,\alpha$), but shown to be very weak in the (p,d) experiment.

i Includes contributions from both 4191 and 4206 keV levels.

Table 4 cont'd.

j Inconsistent with positive parity assignment in $(p,\gamma)^{20}$.

k Inconsistent with an $\ell_p=2$ transition seen in $(d,n)^{26}$.

l Two transitions with $\ell_p=1$ were seen in this region via $(d,n)^{26}$.

m From Price et al.[17].

n Spin assignments based on these states being T=1 analogs of states in ^{26}Mg via comparison of spectroscopic factors.

o Weak transitions, C^2S not extracted in Reference 33.